

Synthesis and Exploration of Tetra-Substituted Porphyrins for Use in a Single-Molecule Organic Solar Cell



WPI

A Major Qualifying Project

Submitted to the Faculty of

WORCESTER POLYTECHNIC INSTITUTE

in partial fulfillment of the requirements for the

Degree of Bachelor of Science in Chemistry

By:

Emma Travassos

Advisor: Ron L. Grimm

Department of Chemistry and Biochemistry

Date: April 25, 2019

This report represents the work of WPI undergraduate students submitted to the faculty as evidence of completion of a degree requirement. WPI routinely publishes these reports on its website without editorial or peer review. For more information about the projects program at WPI, please see <http://www.wpi.edu/academics/ugradstudies/project-learning.html>

Abstract

This report proposes a new organic photovoltaic cell where the light absorber and charge separators are combined on a single molecule. Primarily discussed in this report is the synthesis of the light absorbing molecule, a functionalized porphyrin. We synthesized *trans*-5,15-bis(4-aminophenyl)-10,20-bis(4-carbomethoxyphenyl) porphyrin (TA₂CM₂PP) via a [2+2] condensation with 4-nitrophenyldipyrromethane and 4-carboxymethyl-benzaldehyde followed by oxidation by DDQ to yield *trans*-5,15-bis(4-nitrophenyl)-10,20-bis(4-carbomethoxyphenyl) porphyrin as confirmed by ¹H-NMR. Finally, a tin chloride reduction yielded the desired aminophenyl porphyrin. Silicon surface experiments were conducted with a newly synthesized porphyrin-perylene derivative with zinc coordinated in the porphyrin macrocycle. XP spectra confirm the attachment of porphyrin-perylene derivatives on Si surfaces.

Acknowledgments

I would like to thank the fellow members of the Grimmgroup for all their lab assistance and support, the various CBC professors I've had these past four years for all they've taught me, and of course, my family and friends who've kept me sane through it all. Oh, and special thanks to Professor Grimm for tolerating all clumpy/nonclumpy products.

Table of Contents

Abstract.....	i
Acknowledgements	ii
Table of Contents	iii
List of Figures	iv
1. Introduction	1
2. Background.....	4
2.1 How Do Solar Cells Work?.....	4
2.2 Organic Photovoltaic Cells (OPVs)	5
2.3 An Alternative to the Traditional Organic PV: A Single Molecule Solar Cell	6
2.4 An Introduction to Porphyrins.....	7
2.5 Proposed Single Molecule Solar Cell.....	9
3. Experimental: Preparation of Tethered Surface with Electron Conductor	14
3.1 Preparation of Titanium Dioxide Plates (TiO ₂).....	14
3.2 PTCDA Attachment.....	14
4. Experimental: Preparation of Light Absorbing Molecule.....	16
4.1 Experiments with tetrakis(p-aminophenyl) porphyrin (TAPP).....	16
4.2 An exploration of another synthetic route: Synthesis of <i>trans</i> -diamino/dicarbomethoxy derivative (<i>trans</i> -TA ₂ CM ₂ PP).....	18
5. Experimental: Attachment of light absorber to electron conductor-containing surface.....	24
5.1 Attachment of TAPP to Silicon Surface	24
6. Discussion, Conclusion, and Future Recommendations.....	28
6.1 The Roads Not Taken: Experiments with 5,15-diphenylporphyrin.....	28
6.2 Discussion and Conclusions of Experiments with Tetraphenyl Substituted Porphyrins and Surface Experiments	34
6.3 Future Recommendations.....	36
References	38
7. Appendix A: ¹ H-NMR of CDCl ₃	40

List of Figures

Figure 1.1: Record research efficiencies achieved of kinds of solar cells (1976-2019)

Figure 2.1.1: Components of a typical PV

Figure 2.2.1: Components of an OPV

Figure 2.4.1: Basic Porphyrin Ring

Figure 2.4.2: Delocalization via [18] annulene model in porphyrins

Figure 2.5.1: Structure of *trans*-5,15-bis(4-nitrophenyl)-10,20-bis(4-carbomethoxyphenyl) porphyrin

Figure 2.5.2: Perylene-3,4,9,10-tetracarboxylic dianhydride (PTCDA)

Figure 2.5.3: Structure of 2,2':5',2'':5'',2''':5''',2''''-quaterthiophene

Figure 2.5.4: The proposed single molecule solar cell

Figure 2.5.5: Energy Diagram of the Single Molecule Solar Cell.

Figure 4.1.1: ¹H-NMR Spectrum of tetra(p-nitrophenyl) porphyrin

Figure 4.1.2: ¹H-NMR Spectrum of tetrakis(4-aminophenyl) porphyrin

Figure 4.2.1: Synthetic Route to *trans*-TA₂CM₂PP

Figure 4.2.2: ¹H-NMR Spectrum of 4-nitrophenyldipyrromethane

Figure 4.2.3: ¹H-NMR Spectrum of 5,15-bis(4-carbomethoxyphenyl)-10,20-bis(4-nitrophenyl) porphyrin

Figure 4.2.4: Beta-pyrrole hydrogen peaks in *cis* and *trans*-TN₂CM₂PP

Figure 5.1.1: FTIR Spectrum of PTCDA vs. PTCDA-TAPP product

Figure 5.1.2: FTIR spectrum of PTCDA-TAPP silicon plate

Figure 5.1.3: XPS Data from Sample 1 (no zinc insertion) and Sample 2

Figure 6.0.1: Reaction scheme for the synthesis of 10-aminophenyl-5,15-diphenylporphyrin (product of Kumada coupling)

Figure 6.1.1: TLC Monitoring of synthesis of 5,15-dibromo-10,20-diphenyl porphyrin

Figure 6.1.2: ¹H-NMR Spectrum of 5,15-dibromo-10,20-diphenyl porphyrin

Figure 6.1.3: ¹H-NMR Spectrum of 5-bromo-10,20-diphenyl porphyrin

Figure 6.1.4: ¹H-NMR Spectrum of Zn(5-bromo-10,20-diphenyl porphyrin)

Figure 6.1.5: Desired product of Kumada Coupling

Figure 6.2.1: Comparison of XPS data from zinc and chlorine on surface of sample 2

1. Introduction

With the ongoing global energy and climate crises, it is becoming more important than ever to look towards new forms of renewable energy. Fossil fuels have been the dominant energy source worldwide for over a century and today they still account for nearly 80% of all energy use.¹ Fossil fuels have been closely linked to negative environmental impacts, notably pollution of air and water and global warming. Current research efforts have turned towards looking at alternative renewable energy sources. One of the most popular forms of renewable energy for research is solar, as it utilizes an earth-abundant and unlimited resource to produce energy without carbon emissions.

Solar energy is not a new concept or field. Development of photovoltaic technology can be traced as far back as the Industrial Revolution when French physicist Alexandre Edmond Becquerellar demonstrated the photovoltaic effect. The world's first rooftop solar panel was invented in 1883 by Charles Fritt and Einstein's 1905 paper on the photoelectric effect combined with the studies of Becquerellar led to modern developments of the photovoltaic cell. The first modern PV was manufactured by Bell Labs in 1954 and soon the US military took a keen interest in solar energy to power satellites, however, at the time PVs were considered too costly for commercial industry.¹

The 1970s experienced an emerging energy crisis in America with tightly controlled oil prices and the Arab oil embargo of 1973. In response to these difficulties, Congress passed five energy bills in 1974, and solar energy was cited as a potential solution to the energy crisis.¹² Several institutions were created that aimed to promote solar energy in the US, notably the National Renewable Energy Laboratory (modern name), The Energy Research and Development Administration (ERDA), and the Department of Energy (DOE).¹¹ Though significant strides were made in the 1970s to popularize solar and increase funding of PV and PEC research,¹¹ the conversation about cheap and commercially available solar energy did not occur until the late 1990s and

2000s when photovoltaic conversion of thin-film solar cells began to reach new levels of efficiency and so-called “DIY Solar Panels” began to gain popularity.¹²

Today, there is much ongoing academic research in solar energy and most newly proposed models are third generation PVs, meaning they have the potential to exceed the Shockley–Queisser limit of 31–41% power efficiency for single bandgap solar cells. These models exist only as prototypes and are not yet in the commercial market.

Furthermore, they have the potential to be cheaper, flexible, and easier to produce.¹⁵

Third generation solar technology includes copper zinc tin sulfide (CZTS), perovskite solar cells, dye-sensitized solar cells (DSSCs), and organic photovoltaics (OPVs).¹⁵

Figure 1.1 shows the record research efficiencies achieved by the different kinds of solar cells.

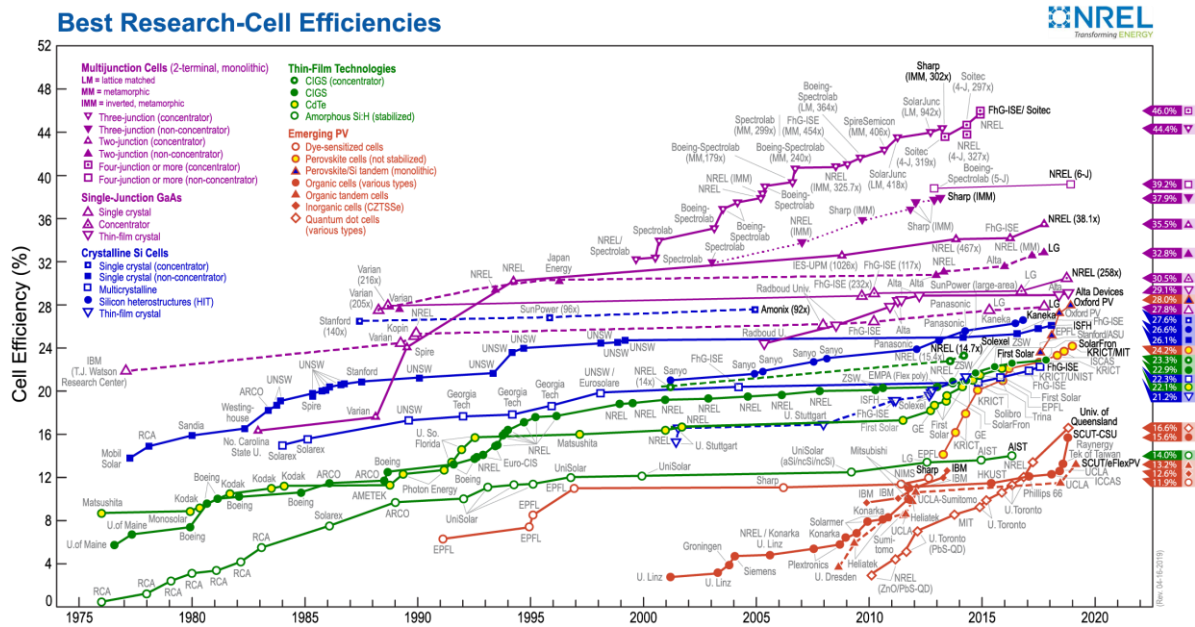


Figure 1.1: Record research efficiencies achieved of kinds of solar cells (1976-2019). When looking at emerging PV one can see that the record efficiency for an OPV is 15.9% and most emerging, or third generation, PVs have efficiencies in the 12%–17% range (apart from perovskites) Data from NREL Best Research-Cell Efficiency Chart (<https://www.nrel.gov/pv/cell-efficiency.html>).

Apart from perovskites, most generation three solar cells have efficiencies that fall around 12–17%. Traditional silicon based solar cells have efficiencies around 20%, however, many generation-three solar cells can be manufactured with less

environmental toxicity and offer unique properties that make them more versatile and applicable to new industries than the rigid and bulky commercially available solar panels of today.¹³

This research explores a new kind of OPV with potential for higher efficiency. One comprised of a single molecule equipped with all necessary components to effectively absorb light, transfer electrons, and generate electric current.

2. Background

2.1 How Do Solar Cells Work?

The basic function of a solar cell is to allow photons (or light) to free electrons from atoms, thus generating a flow of electricity. Solar cells are made up of smaller units called photovoltaic cells (PVs), and these PVs are linked together, making the larger solar cell. PVs must be able to generate an electric field. To make this happen the semi-conductor material, traditionally silicon, must be doped. This means the material is given a positive or negative charge, therefore, the material is then referred to as being n-type or p-type depending on the nature of the doping. Typically, n-type silicon is doped with phosphorus which adds electrons to the material giving it a negative charge. In contrast, p-type silicon is typically doped with boron, lending the material fewer electrons and thus a positive charge.² In a typical solar cell, both n-type and p-type semi-conducting material is present, and the charge differences generate an electric field at the p-n junction between the silicon layers. The presence of the electric field enables a free electron to pass through the silicon junction.²

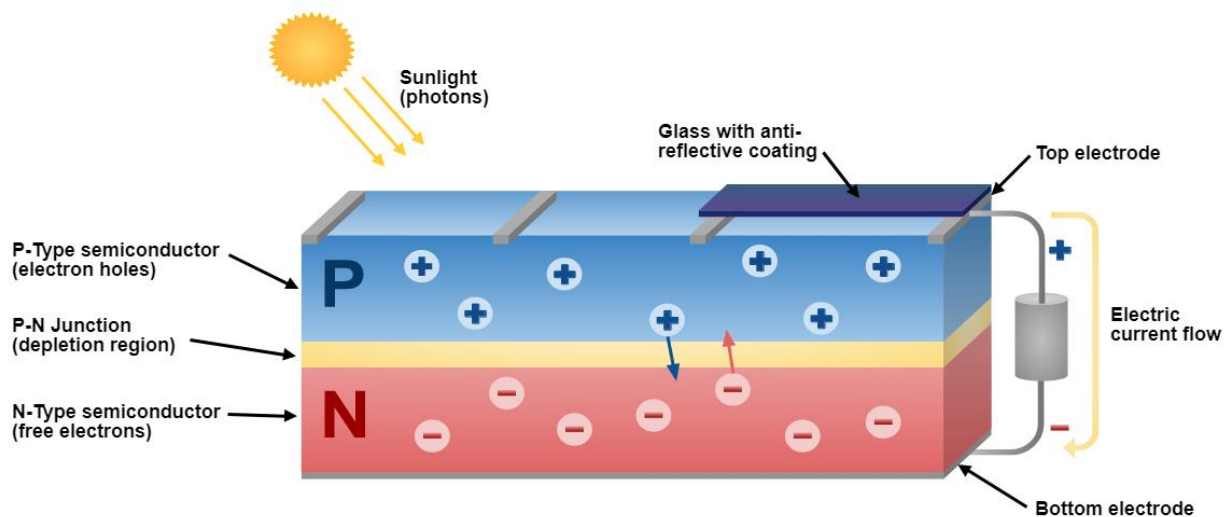


Figure 2.1.1 Components of a typical PV device. All solar cells must be able to absorb light generate free electrons (-) and free holes (+), separate the electrons and holes in space (i.e. a p-n junction)

From <http://www.apricus.com/solar-pv-systems-pv-panels-19.html#.XK9QZehKg2w>

The final necessary component is some sort of conductive plate/contact that can collect electrons and transport them to wires that allow the flow of electrons to generate electricity.²

2.2 Organic Photovoltaic Cells (OPVs)

OPVs have the same basic goal as all other solar cells but offer unique properties and advantages that make them a promising new technology. OPVs can be thin, extremely light, flexible, and manufacturable by traditional roll-printing techniques. Their unique properties make them candidates for application in areas such as aerospace technology and wearable electronics.²

OPVs use molecular or polymeric absorbers to generate a localized excitation. Absorbers are utilized in conjunction with an electron acceptor that has ideal molecular orbital energy states to facilitate electron transfer. When photons are absorbed, they move to the interface between the absorber and acceptor material where the energy differences in the molecular orbitals of the two materials provides the force to generate free charge carriers⁷. These charge carriers are an electron and a hole, which is a position where an electron lacks in an atomic lattice.

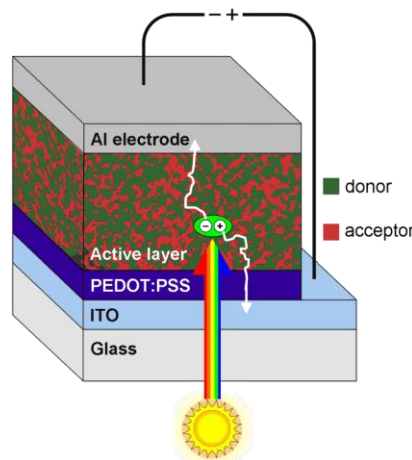


Figure 2.2.1 Components of an OPV. Mixing of the n-type and p-type material in an OPV (see donor/acceptor region) causes efficiency losses because charges can recombine. From DOI 10.1002/adfm.201000975

Though promising, OPVs do have significant issues when it comes to efficiency. Researchers have produced OPVs with efficiencies near 16%, but in reality, many OPVs do not reach this efficiency level.¹⁰ The low efficiencies are related to small exciton diffusion lengths and poor carrier mobilities. Efficient solar cells allow electrical charges to travel through the material quickly. If charges are made to move slower, they can become “stuck” or combine with charges of opposite polarity and recombine.⁷ This can happen in molecular OPVs because molecules do not have the same orderly arrangement as silicon and molecules have a tendency to hold onto charge.⁷ Research has also shown OPVs tend to have a shorter lifetime than traditional solar cells.⁷

2.3 An Alternative to the Traditional Organic PV: A Single Molecule Solar Cell

Electrons moving through a single molecule system can exist in two forms. The first is electron transfer which involves the transfer of electrons from one end of the molecule to the other. The second involves current passing through a single molecule which is “strung” between two electrodes.¹¹ Despite difficulties of a single molecule system such as fluctuations in spectroscopic data, there has been significant progress in recent years with single molecule electrical systems.¹¹

The history of molecular electronics can be traced back to work done by Hans Kuhn in the 1970s who showed through experiments involving monolayers of cadmium salts of fatty acids that conductivity decreased exponentially with monolayer thickness, thus demonstrating electron tunneling through an organic monolayer. Later in 1974, Aviram and Ratner suggested “that a single molecule could act as a device — here a molecular rectifier—and that a single molecule circuit with two electrodes could actually be made and measured.”¹¹ With the advent of the scanning tunneling microscope and atomic force microscope in the 1980s, scientists were able to measure the conductance of single molecules. With these technological advances potential in

molecular electronics was realized, and more research groups began to do studies on these sorts of systems and determine the best ways to carry out these experiments and measurements.

Once the core of the molecule is complete, in most basic terms, it must be attached to a structural component at either end that will bond with an electrode. Many experiments have featured gold or platinum electrodes though there are a variety of other options. The major problems encountered “involve conductance measurements of single molecules, which almost inevitably result in very large fluctuations in experimental data.”¹¹ The best designs for making these sorts measurements are based on the electrochemical or mechanical break junction, as they can make rapid measurements and output easy to analyze data.¹¹ In essence, the single molecule system mimics a semiconductor band structure by taking advantage of electron rich and electron poor regions to achieve conduction through aligned orbitals with respect to the Fermi energy of the electrodes.

To achieve this, our research involves a bottom-up building approach that begins with the synthesis of the desired light-absorbing molecule, a functionalized porphyrin.

2.4 An Introduction to Porphyrins

Porphyrins are a class of macrocyclic organic dyes capable of forming metallic complexes (commonly with Zn, Mg, Ni, Cu, etc.) characterized by the presence of the porphyrin ring structure. This ring is formed from a union of four pyrrolic rings linked by vinyl bridges.⁸

Porphyrins are available for substitution at twelve positions. Eight of these positions are at the β positions (2,3, 7,8 12,13,17,18) on the pyrrolic rings and the other four are at the meso positions (5,10,15,20) on the vinyl bridges. Porphyrins tend to favor tetra meso-substitution and naturally occurring porphyrins are asymmetrically β -substituted.⁸

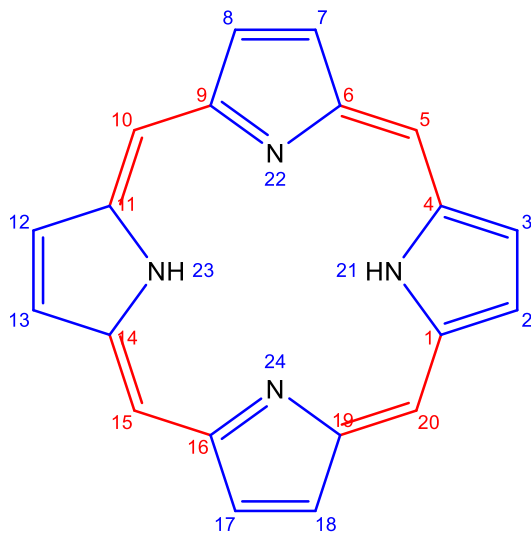


Figure 2.4.1 Basic porphyrin ring. Pyrrolic rings are represented in blue while vinyl bridges are presented in red. Porphyrins can be substituted at 12 positions: the 8 β positions (2,3, 7,8 12,13,17,18) on the pyrrolic rings and the 4 meso positions (5,10,15,20) on the vinyl bridges.

Being organic dyes, porphyrins are generally characterized by significant color intensity. Most porphyrins have intense absorptions in the visible light spectrum though are best characterized by their absorption in the Soret Band (located in the near UV).⁸ Furthermore, porphyrins have aromaticity, as displayed in the macrocyclic delocalization pathway (see Figure 2.4.2) and this property can clearly be observed in ¹H-NMR spectra by the strong downfield shifts of peripheral hydrogens and the strongly (negatively) upfield shifted inner hydrogens.⁸

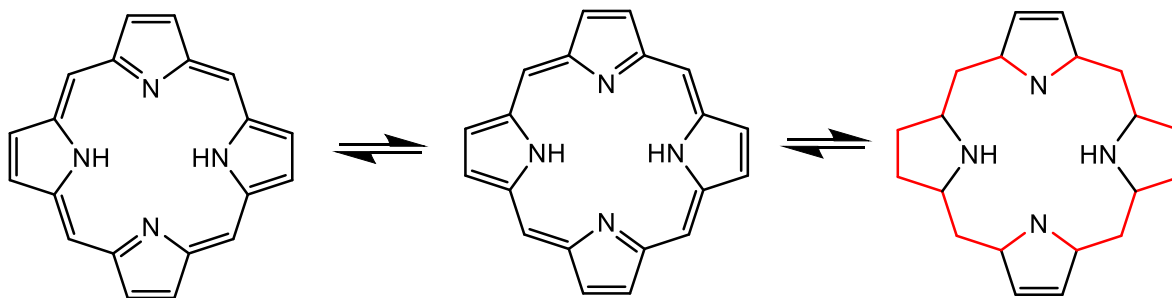


Figure 2.4.2 Delocalization via [18]annulene model in porphyrins

Porphyrins are weak bases, often existing in the free base form where the two internal hydrogens move between the inner four nitrogen atoms. The *trans* tautomer (21,23 H) is energetically preferred to the *cis*.⁸ The properties of being a strong light absorber and the presence of a delocalized π system make porphyrins a candidate for use in a proposed single molecule solar cell as a light absorber.

2.5 Proposed Single Molecule Solar Cell

We hypothesize that combining the p-type material, the light absorber, and the n-type material into a single molecule will yield more efficient solar-energy conversion than traditional molecular organic PV as it can eliminate the efficiency losses experienced in traditional OPVs due to the donor and acceptor material being combined in the same region of the cell.

As highlighted in § 2.4, porphyrins provide a unique structure that lends itself to having electrical properties that are desirable in this type of single molecule system. Porphyrins contain a versatile conjugated macrocyclic system that gives them the property of being candidates for usage in organic photovoltaic devices as a light absorbing molecule. Existing photoelectric work often couples fullerenes with porphyrins to create artificial photosynthetic systems and some OPVs. However, it is vital that the porphyrin is appropriate in structure such that exciton diffusion is enhanced, and charge separation can take place.¹⁷ Furthermore, porphyrin research has shown that oxidative and electropolymerization and deposition of conductive porphyrin films is possible and offers the characteristic of being easy to control.¹⁷

We believe that tetra-phenyl substituted porphyrins offer a molecular framework that is ideal for our single-molecule organic PV, particularly those with aminophenyl substituents. Existing research has seen success in using tetra-substituted porphyrins for thin polyporphyrin films on FTO and ITO surfaces and they are notable for their electrochemical properties.¹⁷ It was shown that two aminophenyl substituents can exhibit a hyperporphyrin spectrum with the porphyrin macrocycle, thus creating an excited state charge transfer from the aminophenyl nitrogen to the nitrogens at the center of the macrocycle.¹⁷ Much of this research has been conducted using tetrakis(p-aminophenyl)porphyrin (TAPP), however, as previously stated, it is our intention to attach both a perylene and hole conducting material to the 5 and 15 aminophenyl substituted positions of the porphyrin. Therefore, it is advantageous to us to protect

from reaction at the 10 and 20 meso positions of the porphyrin to ensure that neither the perylene or hole conductor attaches at these positions. Therefore, we desire an asymmetric design. The carbomethoxyphenyl substituent would not react with the perylene or the hole conductor and would not be susceptible to severe oxidation (could see conversion to the carboxylic acid, but this is not concerning). Therefore, the desired porphyrin for this research is *trans*-5,15-bis(4-aminophenyl)-10,20-bis(4-carbomethoxyphenyl) porphyrin (*trans*-TA₂CM₂PP) (see Figure 2.5.1), as it possesses all the structural properties desirable for this research and has a synthetic route that utilizes commercially available starting materials.

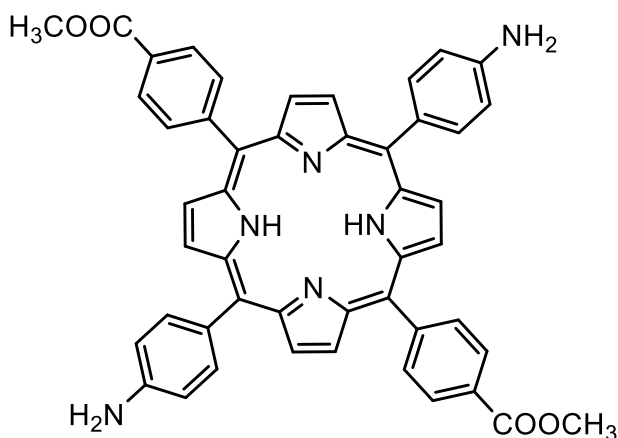


Figure 2.5.1 Structure of *trans*-5,15-bis(4-aminophenyl)-10,20-bis(4-carbomethoxyphenyl) porphyrin. This is the desired porphyrin molecule for the proposed single molecule solar cell.

To form a system capable of conducting current to this light absorbing molecule, other features must be bonded. The first being an “electron conductor” and the second a “hole conductor” to form the complete unit that can be attached to the surface tether.

The electron conductor will be an organic dye, perylene-3,4,9,10-tetracarboxylic dianhydride (PTCDA) (Figure 2.5.2).

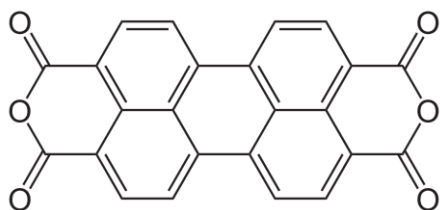


Figure 2.5.2 Perylene-3,4,9,10-tetracarboxylic dianhydride (PTCDA).

PTCDA is a robust molecule and is commercially available. The aromaticity in the perylene compound allows for efficient carrier transport, as the π -electron systems of the carbon double bonds are in contact.¹⁶ However, there are significant barriers when it comes to solubility. Work done by Kelber *et al.* explored a procedure for perylenes using alcohols and 1,8-Diazabicyclo[5.4.0]undec-7-ene (DBU) that produces a ring-opened di-ester di-acid intermediate in solution which is more reactive with the amine and has improved ability to adhere to a surface.⁶

There must also be a hole conducting molecule in the solar cell. The hole conducting material prevents charges from recombining and dampening the efficiency of the cell. A potential candidate for use in our cell is 2,2':5',2'':5'',2''':5''',2''''-quaterthiophene (Figure 2.5.3). Research has shown quaterthiophene to be a good material for use in OPVs as it has generally favorable solubility and considerable absorption in the UV-visible spectrum. Furthermore, the length of the molecule (~1.6 nm) is sufficient to eliminate electron tunneling from the porphyrin through the thiophene itself.

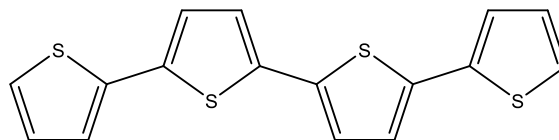
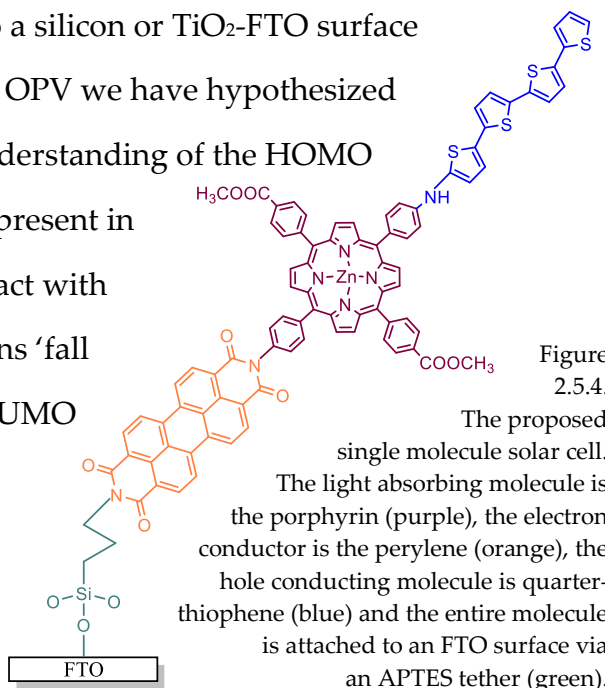


Figure 2.5.3. Structure of 2,2':5',2'':5'',2''':5''',2''''-quaterthiophene.

All these elements combined and attached to a silicon or TiO₂-FTO surface provide the schematic of the single molecule OPV we have hypothesized (Figure 2.5.4). This design is based off an understanding of the HOMO and LUMO levels of each molecular species present in the single molecule OPV and how they interact with electrochemical contacts. Simply put, electrons ‘fall down’ and holes ‘fall up.’ The HOMO and LUMO levels relative to those of the light absorbing molecule must be positioned correctly for carrier selective transport. The electron conducting material needs to have a



HOMO significantly lower than that of the light absorbing molecule and a LUMO only slightly lower than that of the light absorber. In contrast, the hole conducting material needs to have a LUMO significantly higher than that of the light absorber and a HOMO only slightly higher. Furthermore, there needs to be a contact with a low work function (on par with the energy of the LUMO of the electron conductor) and a contact with a high work function (on par with the energy of the HOMO of the hole conductor (see Figure 2.5.5).

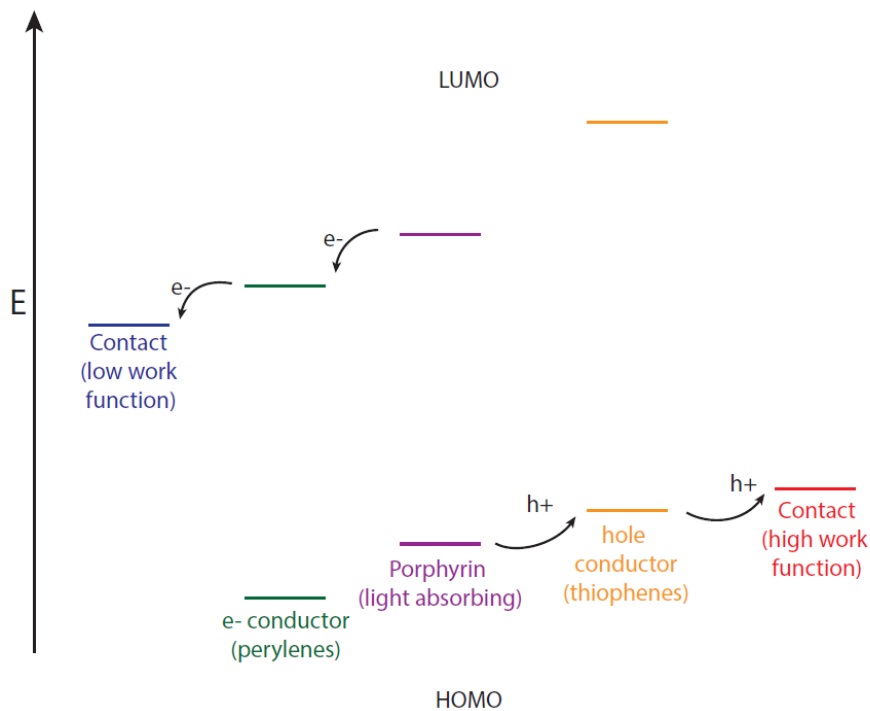


Figure 2.5.5 Energy Diagram of the Single Molecule Solar Cell. Energy is relative. Energy levels must be arranged so that electrons can fall down, and holes can fall up. The relative energies of the HOMO and LUMO of the electron and hole conducting materials are designed so that the states are controlled, and holes and electrons can only travel in one direction.

Achieving the goal of this research first begins with exploration of the light absorbing molecule, the porphyrin, which is the focus of this Major Qualifying Project. The light absorber for this single-molecule design must have a high coefficient of extinction (ϵ), meaning it is a strong absorber of light. Both the perylene and thiophene molecules can absorb light, so it is essential that the porphyrin can absorb significantly more light and be able to achieve the desired asymmetric charge transfer shown in Figure 2.5.5. Synthesis of the desired porphyrin therefore was carried out with these electrochemical and optoelectrical properties in mind along with the molecular structure and reactivity.

3. Experimental: Preparation of Tethered Surface with Electron Conductor

One contact for the single molecule solar cell will be a conductive surface such as silicon or TiO₂ coated FTO. This section explores preparation of TiO₂ plates and a procedure for attaching perylenes, notably PTCDA, to the surface. No surface experiments were done on TiO₂ for this research, but an understanding of how to prepare these plates and attach perylene based species is important, as TiO₂ will be explored for use in our OPV in the future.

3.1 Preparation of Titanium Dioxide Plates (TiO₂)

The preparation of the plates began with the creation of a 0.1 M titanium isopropoxide solution (0.15 mL isopropoxide in 5 mL isopropanol). This solution was left to sit while the fluorine doped tin oxide (FTO) surface was sonicated in acetone, isopropanol, and water, each for a duration of 5–10 min. Following sonication, the FTO plates were placed in a 100–120 °C oven for 15–20 min or until dry. Once dry, the plates were spin coated with the 0.1 M titanium isopropoxide. The plates were subsequently placed in a 500 °C oven overnight.

Once the TiO₂ was successfully deposited onto the FTO surface, the plates were plasma cleaned and ready for silane attachment. 3-aminopropyl triethoxysilane (APTES) was combined with anhydrous toluene (~20 mL toluene and 120 μL APTES). This solution along with a TiO₂ plate was placed in a test tube and heated at 60 °C in an oil bath for 4 hr. After 4 hr the plates were rinsed with toluene and sonicated in toluene and methanol and dried with argon.

3.2 PTCDA Attachment

The perylenation procedure⁶ for TiO₂ is intended to half-open the perylene to aid in surface attachment. Dimethylformamide (DMF) (2 mL), 1-butanol (200 μL), 1,8-Diazabicyclo[5.4.0]undec-7ene (DBU) (160 μL), and PTCDA (144 mg) were combined

and stirred at room temperature. After 30 min, 18 mL of DMF was added to the solution to create a final volume of 20 mL. Each plate intended to have the perylene attachment was placed individually into a test tube and enough solution to completely submerged the plate was added. The tubes were placed in a 60 °C oil bath and left for three days. After three days the perylene solution was discarded (a color change from red to blue/green was observed) and the plates were rinsed with acetone and subsequently sonicated in acetone, methanol, and distilled water (x2) each for 10 min.

4. Experimental: Preparation of Light Absorbing Molecule

Synthesis of the single molecule solar cell begins with exploring different tetra-substituted porphyrins as candidates. Ensuring that a proper porphyrin is selected is essential for the success of this research, as the entire cell is built from reacting with the porphyrin and the design is based off a relative understanding of the HOMO and LUMO levels of porphyrins. As previously stated, it is desirable to have the porphyrin possess an aminophenyl group at the 5 and 15 positions and a different functional group at the 10 and 20 positions that is not able to participate in a condensation reaction with the perylene or thiophene.

Despite not having the intended asymmetric design, tetrakis(p-aminophenyl) porphyrin (TAPP) was also synthesized and used in surface experiments with silicon to explore the success of reacting the perylene with an aminophenyl group and that molecule's ability to attach to a silicon surface. This was done because the synthetic route to TAPP is more straightforward than *trans*-TA₂CM₂PP and allowed us to expedite the surface experiments. These surface experiments are discussed in chapter 5 while this section explores the synthesis of both TAPP and the desired porphyrin *trans*-TA₂CM₂PP.

4.1 Experiments with tetrakis(p-aminophenyl) porphyrin (TAPP)

This synthetic approach begins with synthesis of tetrakis(p-nitrophenyl) porphyrin (TNPP). The goal of this synthetic procedure was to successfully reduce the nitro groups on the porphyrin to the amine to obtain tetrakis(p-aminophenyl)porphyrin (TAPP) and then attempt surface attachment.

4.1.1 Synthesis of tetrakis(p-nitrophenyl) porphyrin (TNPP)

Synthesis of TNPP followed a literature procedure.⁴ Pyrrole was freshly distilled prior to use. Nitrobenzaldehyde (0.500 g, 0.0033 mol) and pyrrole (0.22 mL, 0.033 mol) were

combined in propionic acid and left to reflux for 24+ hr and the flask was subsequently left to sit for 48+ hr. The reaction mixture was then vacuum filtered and a black/purple solid was obtained. The product was washed with methanol and water until no residual propionic acid scent was detectable. The product was purified by column chromatography (chloroform/acetone, 50:50). Two bands were eluted, a brief pale-yellow fraction followed by a large band of a medium brown color. The brown fractions were indicative of the product and were recovered. The product was analyzed by $^1\text{H-NMR}$ (see Figure 4.1.1).

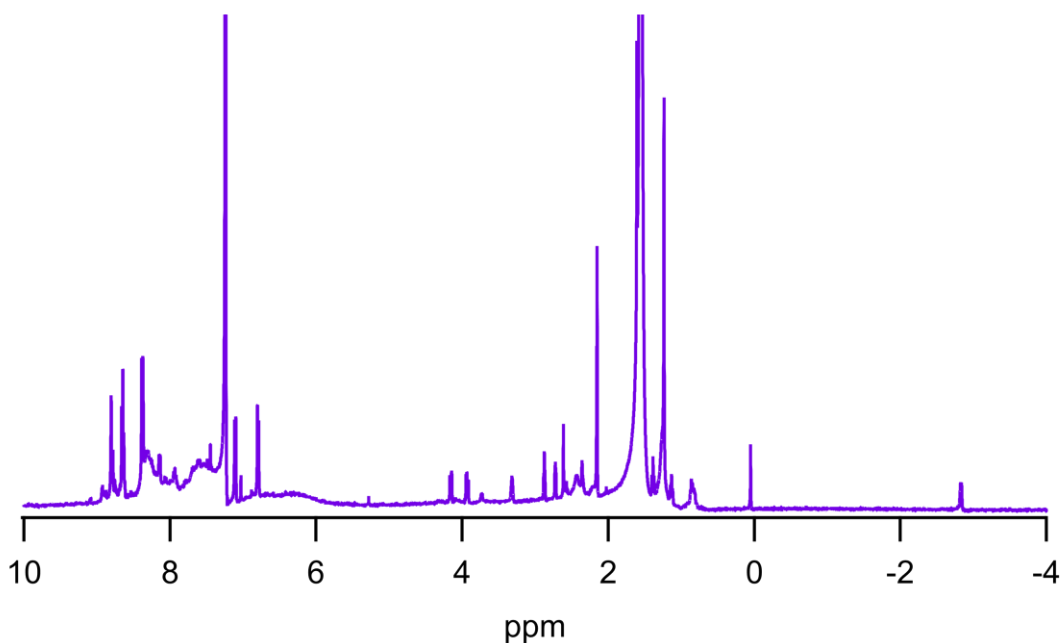


Figure 4.1.1 $^1\text{H-NMR}$ Spectrum of tetrakis(*p*-nitrophenyl) porphyrin (CDCl_3 , CDCl_3): δ 8.81 (s, 8H), 8.66 (d, 8H), 8.38 (d, 8H), -2.81 (s, 2H). The location of the proton features indicates successful synthesis of TNPP, notably the peak for the ArH at 8.66.

4.1.2 Reduction of tetrakis(*p*-nitrophenyl) porphyrin to tetrakis(4-aminophenyl) porphyrin (TAPP) via Tin Chloride (SnCl_2)

This step followed a separate literature procedure.⁵ To a mixture of TNPP (180 mg) in concentrated HCl (7.5 mL) a solution of SnCl_2 (549.9 mg in 2 mL HCl) was added dropwise under argon atmosphere. After stirring at room temperature for 2.5 hr, the

reaction mixture was heated to 80°C for 1 hr and then chilled to 0°C in an ice bath. The mixture was neutralized with ammonium hydroxide at 0°C and a green solid was obtained after vacuum filtration and dispersion in a solution of sodium hydroxide (aq). The product was then vacuum filtered once more and dried in the oven overnight. Once dry, the product was analyzed by ¹H-NMR (Figure 4.1.2). This porphyrin was then used in more experiments detailed in Chapter 5.

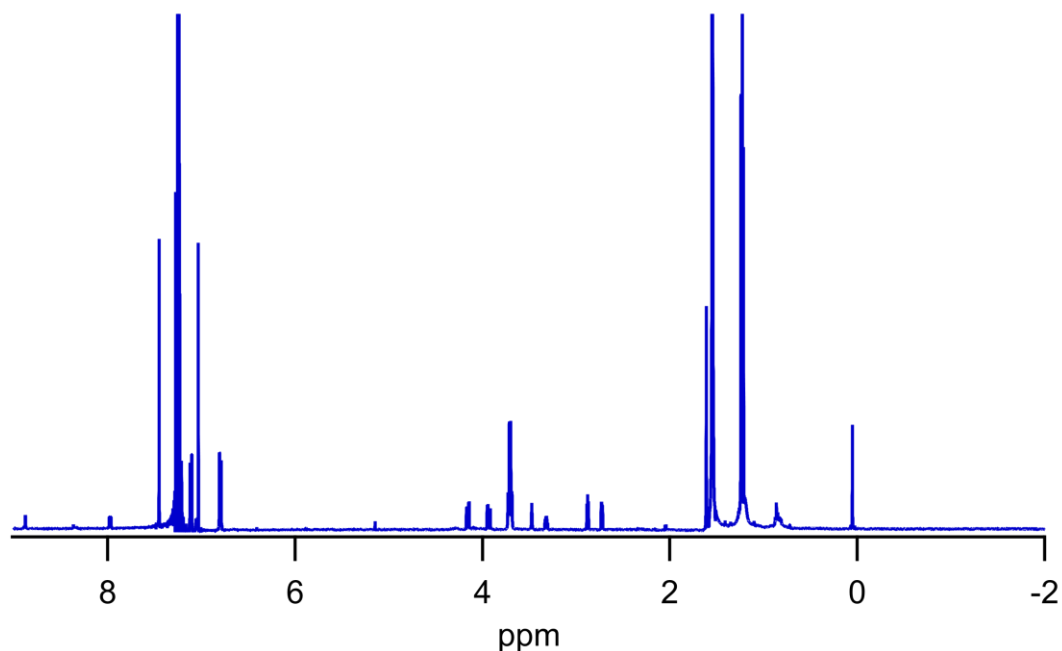


Figure 4.1.2 ¹H-NMR Spectrum of tetrakis(4-aminophenyl) porphyrin in CDCl₃ (note, wide proton NMR was not performed so peak at ~-2.71 (s, 2H, pyrrole H) is not shown) 8.90 (s, 8H, pyrrole ring), 7.987 (d, 8H, ArH), 7.07 (d, 8H, ArH), 3.97 (s, 8H, NH₂). Presence of peaks at 3.97 show successful conversion from the nitro group to the amine.

4.2 An exploration of another synthetic route: Synthesis of *trans*-diamino/dicarbomethoxy derivative (*trans*-TA₂CM₂PP)

Literature by Walters *et al.*¹⁷ describes usage of *trans*-TA₂CM₂PP in dye-sensitized TiO₂ solar cells. As previously stated, this molecule is attractive for this research as the carbomethoxyphenyl groups are at the 10,20 positions and the aminophenyl at the 5 and 15.

With the amino groups being at two positions, instead of four as in TAPP, surface attachment can be more regulated and occurrences of attachments at multiple amino groups on the surface can be avoided. This structure more closely resembles that of the diphenyl porphyrin (DPP) this research originally began with and may possess the same desired electronic properties.

This molecule will be synthesized following the synthetic route in Figure 4.2.1.

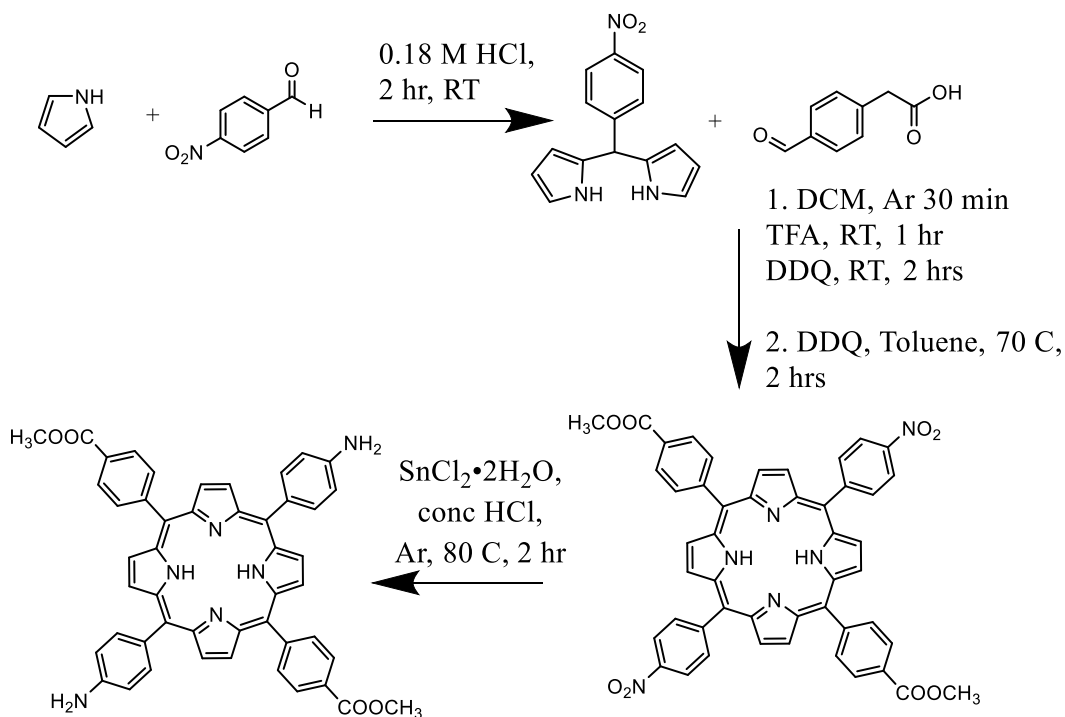


Figure 4.2.1 Synthetic Route to *trans*-TA₂CM₂PP. The synthetic route begins with the synthesis of 4-nitrophenyldipyrromethane followed by a [2+2] condensation with 4-carboxymethyl-benzaldehyde. The intermediate product is then oxidized to oxidation yield the nitro/carbomethoxy phenyl porphyrin. Finally, reduction of the nitro group by tin chloride gives the desired product.

4.2.1 Synthesis of 4-nitrophenyldipyrromethane

Making the nitrophenyldipyrromethane precursor is the first step of this synthesis.¹⁹ Pyrrole (37 mL) was freshly distilled and added to 100 mL of 0.18 M HCl followed by the addition of 4-nitrobenzaldehyde (2.0g). The resulting mixture was stirred at room temperature for 2 hr. A color change from a bright yellow to a deeper orange-yellow

was observed. The precipitated solid was collected by vacuum filtration (additional HCl may need to be added to encourage precipitation). The solid was washed with water and diethyl ether and then recrystallized from methanol. A bright yellow solid was produced in good yield and analyzed by $^1\text{H-NMR}$ spectroscopy (see Figure 4.2.2).

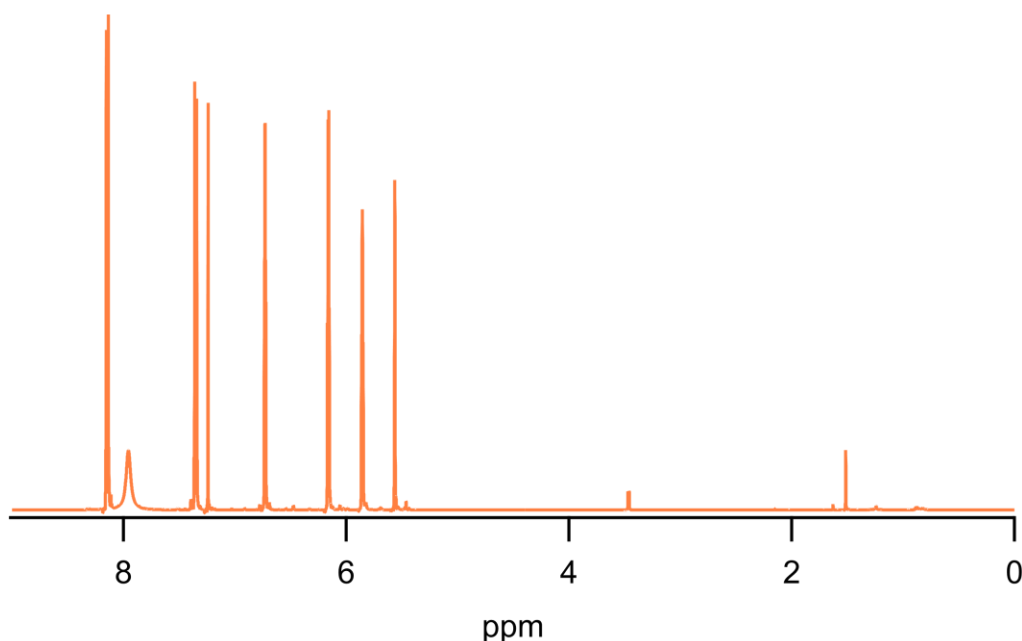


Figure 4.2.2 $^1\text{H-NMR}$ spectrum of 4-nitrophenyldipyrromethane in CDCl_3 : 8.19 (d, $J = 6$ Hz, 2H), 7.95 (bs, 4H, 2H), 7.39 (d, $J = 6$ Hz, 2H), 6.76 (q, 2H), 5.90 (m, 2H), 5.59 (s, 1H, meso-H)

4.2.2 Synthesis of 5,15-bis(4-carbomethoxyphenyl)-10,20-bis(4-nitrophenyl) porphyrin (TCM₂N₂PP)

This procedure comes from a publication by Milanesio *et al.*⁹ Previously synthesized 4-nitrophenyldipyrromethane (0.547g, 0.002 mol) and 4-carboxymethylbenzaldehyde (0.322g, 0.002 mol) were combined in DCM (100 mL) and argon was bubbled through the mixture for ~30 min. Following, while still bubbling with argon, trifluoroacetic acid (TFA) (0.245 mL) was added slowly to the reaction mixture and was left stirring at room temperature for 0.75–1 h. Upon addition of the TFA, the reaction mixture turned from a pale yellow to a deep red.

After the allotted time, 2,3-dichloro-5,6-dicyano-1,4-benzoquinone (DDQ) (0.454g, 0.002 mol) was added and the reaction was again left bubbling with argon and stirring at room temperature for an additional 2 hr. The reaction mixture was then vacuum filtered through Celite and the product was eluted with copious DCM. The solvent was then removed by rotary evaporation and a deep green/black intermediate product was recovered.

All the intermediate and an additional 0.002 mol of DDQ were combined in toluene (25 mL) and heated to 70°C for 2 hr. The reaction mixture was again vacuum filtered through Celite and eluted with DCM. Upon removal of the solvent by rotary evaporation, a purple/black solid was obtained (0.617g). This product (TCM₂N₂PP) was recrystallized in methanol and characterized by ¹H-NMR.

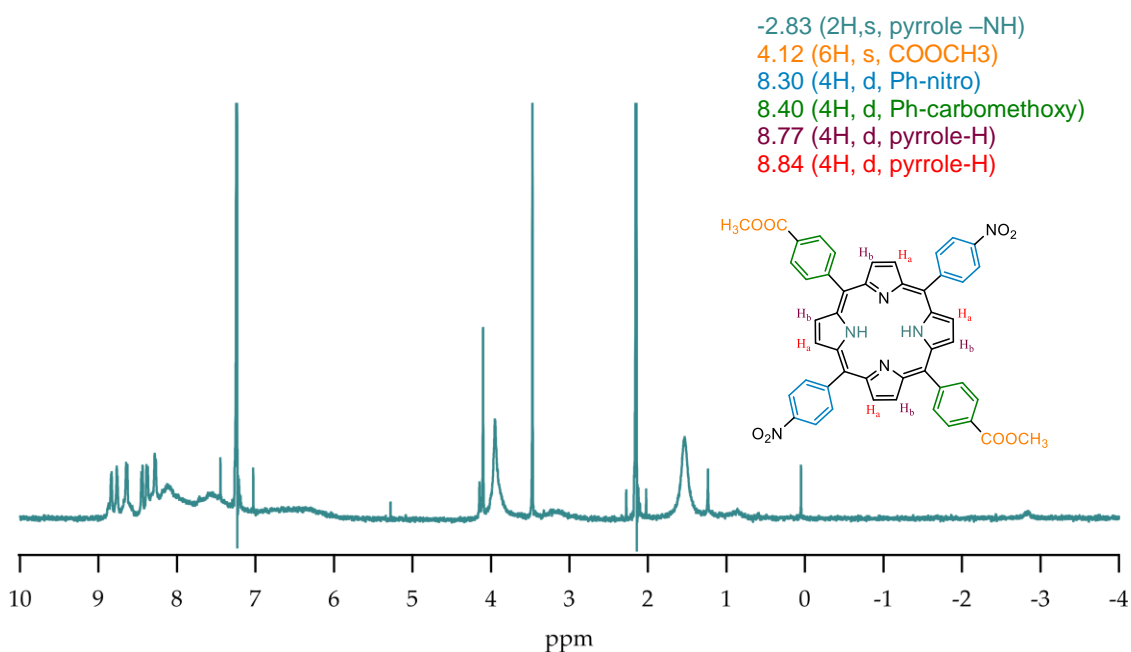


Figure 4.2.3 ¹H-NMR Spectrum of 5,15-bis(4-carbomethoxyphenyl)-10,20-bis(4-nitrophenyl) porphyrin in CDCl₃ -2.83 (2H,s, pyrrole -NH), 4.12 (6H,s, COOCH₃), 8.30 (4H, d, Ph-nitro), 8.40 (4H, d, Ph-carbomethoxy), 8.79 (4H, d, pyrrole-H), 8.86 (4H, d, pyrrole-H). Superfluous peaks are mostly a result of contamination in the CDCl₃. See

Appendix A for CDCl₃ NMR spectra.

Previous research has indicated that the *cis* isomer of this compound does not deposit well onto a surface,¹⁸ so before moving to the next step of the synthesis, it was confirmed that the *trans* isomer was the product obtained in the previous synthesis. The stereochemistry becomes fixed by this point in the synthesis. The *trans* isomer is characterized by the ¹H-NMR peaks for the beta pyrrole hydrogen appearing as doublets. In the *cis* isomer, these hydrogens appear as triplets.¹⁸

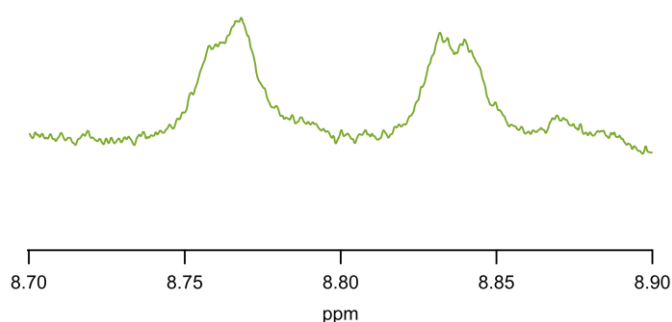


Figure 4.2.4 beta-pyrrole hydrogen peaks in *cis* and *trans*-TN₂CM₂PP. Doublet features are indicative of the *trans* isomer.

Expansion of the region where the beta-pyrrole hydrogen peaks lie in the nitro porphyrin intermediate revealed a series of doublet peaks characteristic of the *trans* isomer.

4.2.3 Reduction to 5,15-bis(4-carbomethoxyphenyl)-10,20-bis(4-aminophenyl) porphyrin

Similar to the reaction detailed in §4.1.2,⁵ *trans*-TN₂CM₂PP was reduced to the aminophenyl porphyrin via a SnCl₂ reduction. The porphyrin (0.133 g) was dissolved in concentrated HCl (10 mL) and SnCl₂ (370 mg) was introduced argon atmosphere. After stirring at room temperature for 2.5 hr, the reaction mixture was then heated to 60 °C and left overnight. The next day, the reaction mixture was chilled to 0 °C and neutralized with sodium hydroxide. A dark black/purple solid was obtained via

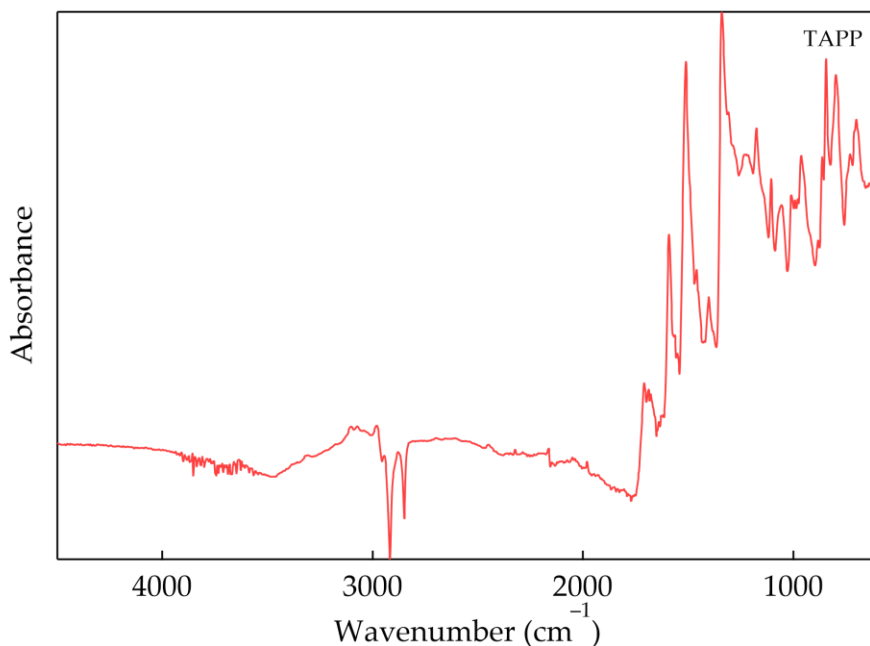
vacuum filtration in low yield. The $^1\text{H-NMR}$ revealed that this synthesis did not produce the desired porphyrin possibly because of a low quantity of starting material and the fact that the batch of $\text{TN}_2\text{CM}_2\text{PP}$ used for this reduction attempt was not verified by $^1\text{H-NMR}$ to be the *trans* product. It is recommended to repeat this same synthetic procedure but with higher quality *trans*- $\text{TN}_2\text{CM}_2\text{PP}$, as this procedure was successful at reducing TNPP to TAPP .

5. Experimental: Attachment of light absorber to electron conductor-containing surface

5.1 Attachment of TAPP to Silicon Surface

Previously synthesized TAPP product was reacted with PTCDA to create a porphyrin-
perylene derivative. The first step of this involves opening the perylene in a manner
very similar to the procedure described in §3.1.2. PTCDA (0.912 g) was combined with
DMF (6 mL), ethanol (0.75 mL) and DBU (0.895 mL) and placed in an oil bath at 60 °C
for 3 hr.⁶ Following the 3 hr, the solution changed color from a bright red to a deeper
reddish blue color. This mixture was stored under a nitrogen balloon as it is air
sensitive.

The following day, all TAPP product was added to the mixture and once again
left in an oil bath at 60 °C overnight. The mixture was then vacuum filtered and
analyzed by FTIR.



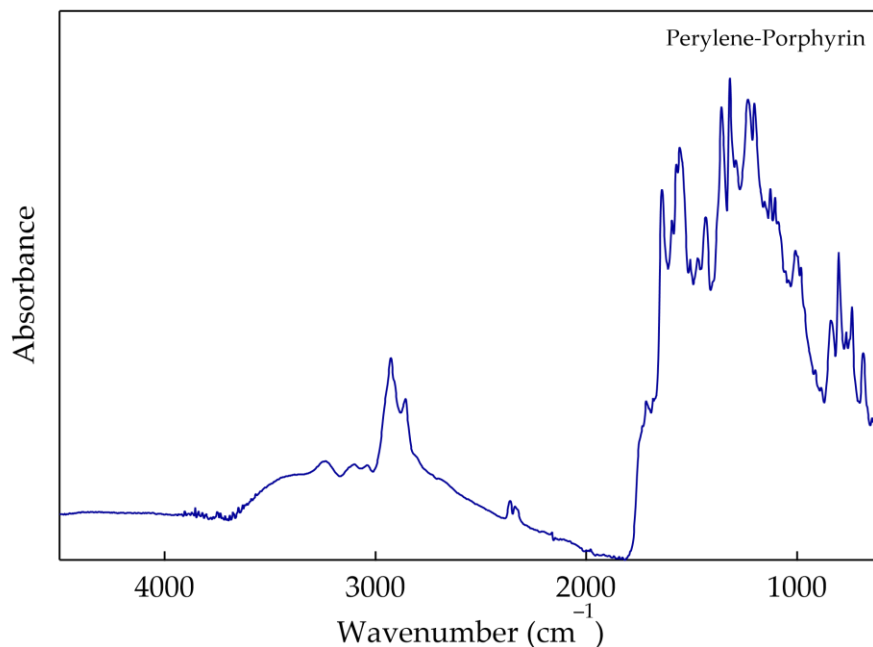


Figure 5.1.1 FTIR Spectrum of PTCDA (top) vs. PTCDA-TAPP product (bottom). Appearance of new features, disappearance of some porphyrin features and shifts of porphyrin peaks suggest the synthesis of a new compound.

More intensive and higher quality IR needs to be taken.

Next, the PTCDA-TAPP product was attached to a silicon surface. Double sided polished n-silicon was APTES attached following the procedure described in §3.1.1. The PTCDA-TAPP perylene opening solution as previously described in this section was made and the silicon plate was placed into this solution and left at 80°C in an oil bath for 48 hr. The plate was rinsed with acetone and subsequently sonicated in acetone, methanol, and distilled water (×2) each for 10 min. The plate was then stored in a 100 °C oven. FTIR characterization was done of this plate (see Figure 5.1.2)

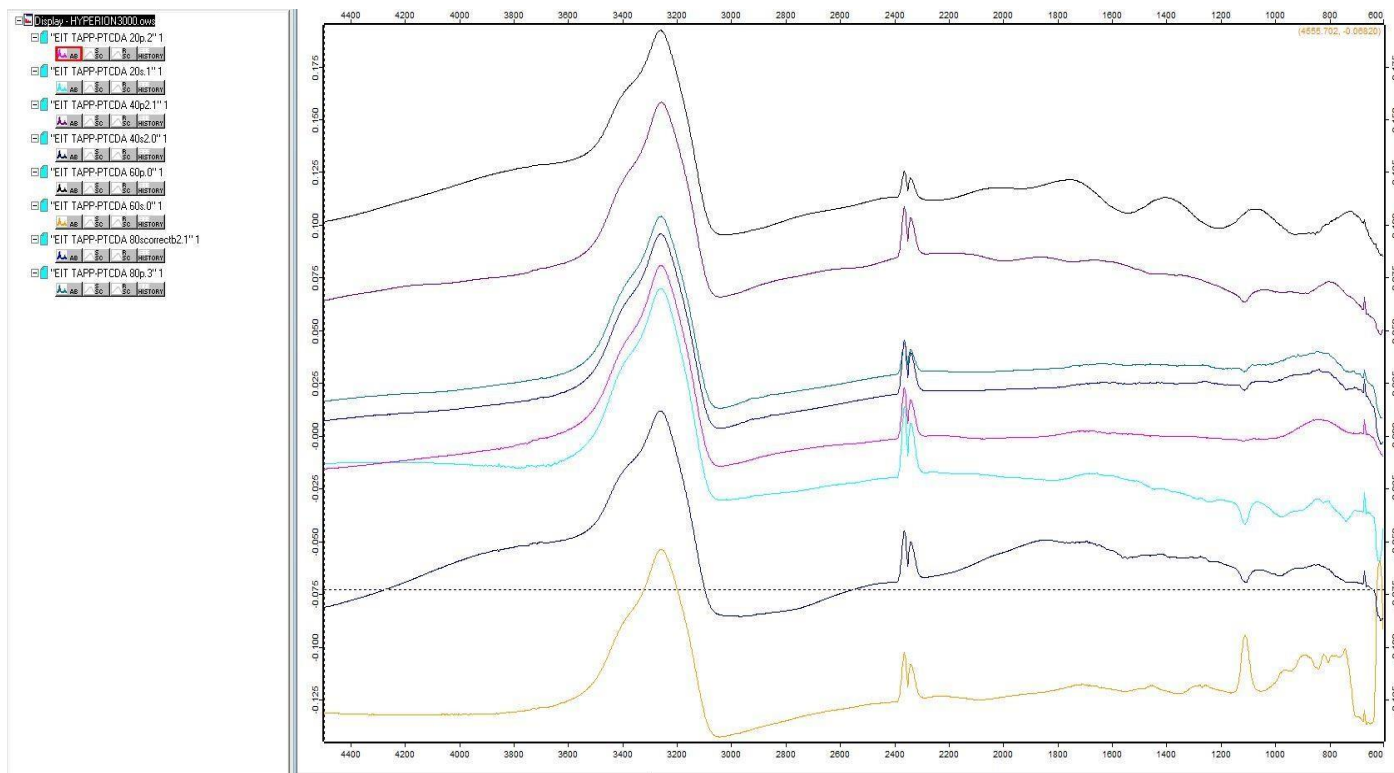


Figure 5.1.2: FTIR spectrum of PTCDA-TAPP silicon plate. Backgrounds of silicon plates were taken prior to surface attachment of the PTCDA-TAPP. Spectra were taken at angles 20°-80° (every 20°) with both s and p polarization and 512 scans/min

From these scans it was difficult to determine whether attachment was successful. When FTIR analysis was performed, the spectra were obtained with 512 scans, which is not precise enough to clue in on the stretches that confirm perylene attachment (imide stretch ~ 1650 cm⁻¹ and phenyl stretch ~ 1592 cm⁻¹).

Two silicon plates with the PTCDA-TAPP attachment were analyzed by x-ray photoelectron spectroscopy (XPS). One plate (sample 1) did not have zinc inserted into TAPP. The second plate (sample 2), did. The zinc was inserted by placing the plate in an aqueous zinc chloride solution and warming it to 60 °C for 24 hr. The plates were then scanned for carbon, nitrogen, oxygen, silicon, and zinc. Sample 2 was also scanned for chlorine (Figure 5.1.3).

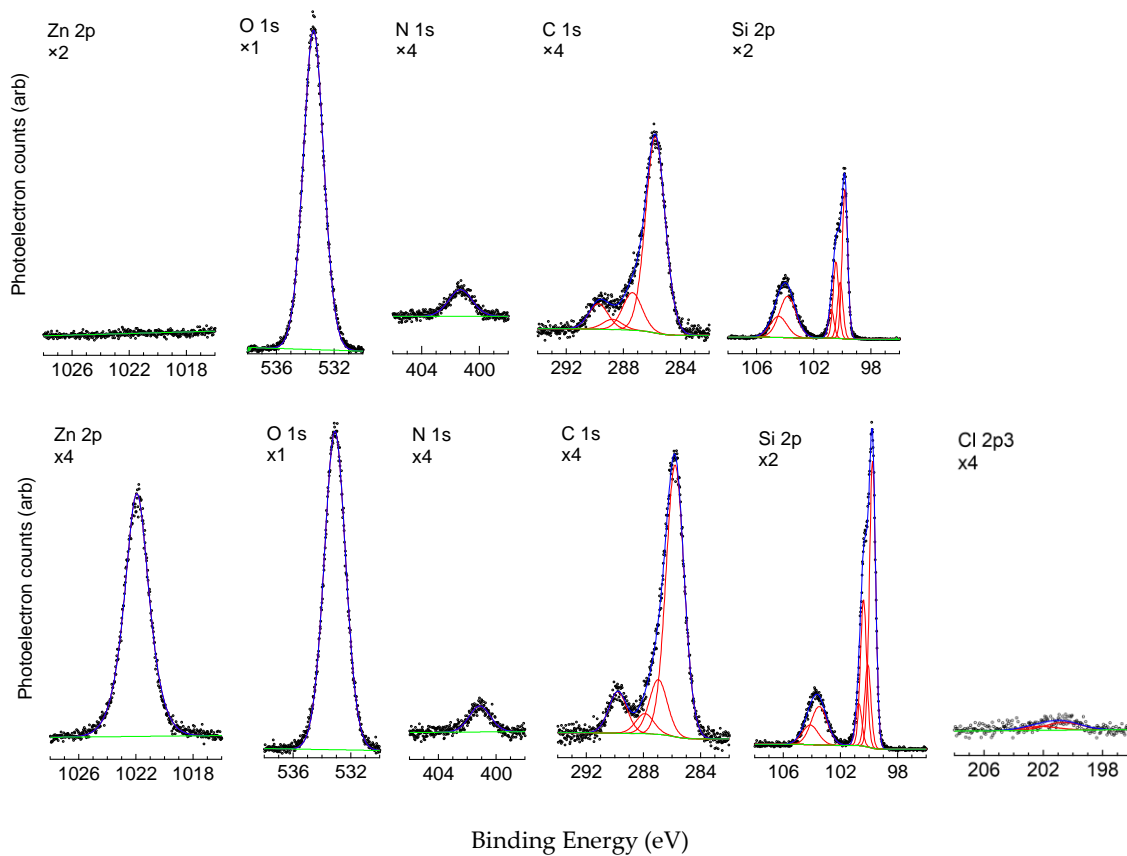


Figure 5.1.3 XPS Data from Sample 1 (no zinc insertion, top) and Sample 2 (bottom) Results show that the attachment of the perylene-porphyrin derivative was successful, and that zinc can be inserted into the porphyrin post surface attachment.

6. Discussion, Conclusion, and Future Recommendations

In this section, we discuss previous synthesis attempts utilizing and derivatizing commercial porphyrins, namely 5,15-diphenyl porphyrin, why the Walter synthesis was ultimately utilized, the impact of the silicon surface experiments, and the implications for the continuation of this project by a future researcher or MQP student.

6.1 The Roads Not Taken: Experiments with 5,15-diphenylporphyrin

5,15-diphenylporphyrin (DPP) was originally selected as the starting material for this research as its structure was already in a desirable form where it could be functionalized at the available 10 and 20 positions. The original intent was to perform a Kumada coupling at one position of the molecule to attach an aniline group and then attach a hole conducting material at the other available spot. Research down this path only proceeded as far as completing one attempt at performing the Kumada coupling before other more successful routes were taken. Figure 6.1.1 displays the overall reaction scheme for the chemistry that was performed using DPP.

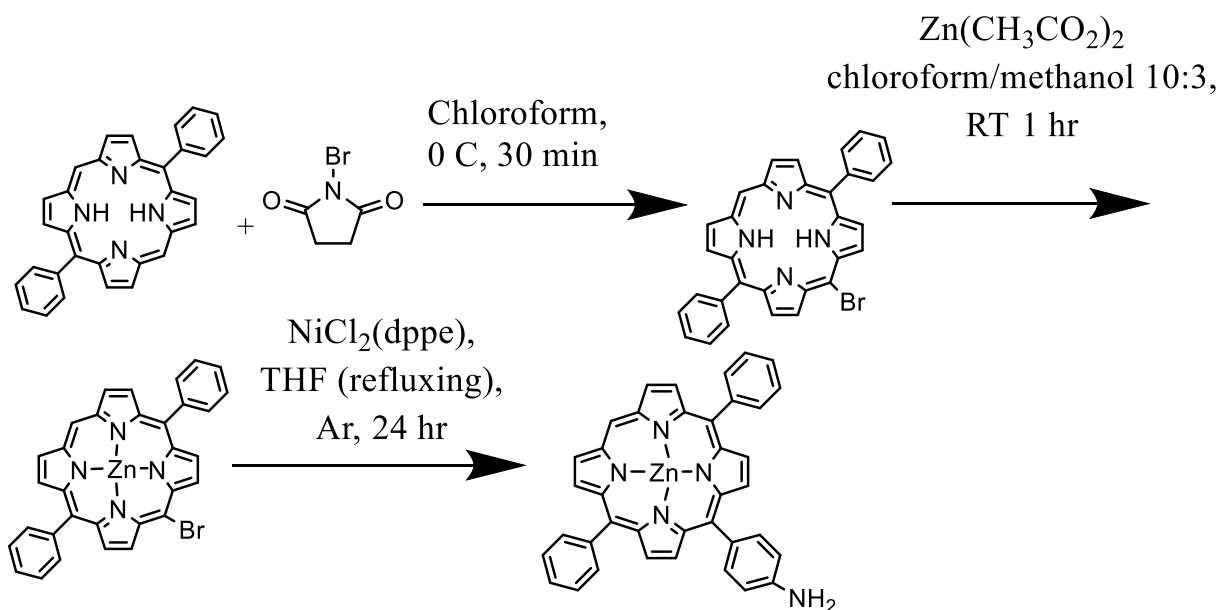


Figure 6.1.1 Reaction scheme for the synthesis of 10-aminophenyl-5,15-diphenylporphyrin (product of Kumada coupling). Synthesis begins with bromination of DPP, followed by zinc insertion, and then the Kumada coupling.

6.1.1 Halogenation and Kumada Coupling Reaction with DPP

To begin work on the synthesis of the desired porphyrin, halogenation of DPP at the 10 and 20 positions was first attempted. This synthesis was based off the synthesis for the same molecule published by DiMagno *et al.*³ To achieve dibromination of DPP, a round bottom flask containing chloroform was first cooled to approximately 0°C in an ice bath. 5,15-diphenylporphyrin and N-Bromosuccinimide (NBS) along with a small amount of pyridine (to act as an acid scavenger) were then added to the cold chloroform and allowed to react for 30 min. Upon first attempt of this synthesis, the reaction was monitored by TLC (3:1 Hexane/Toluene used as eluent) to determine the appropriate length of time to allow for product formation (See Figure 6.1.1)

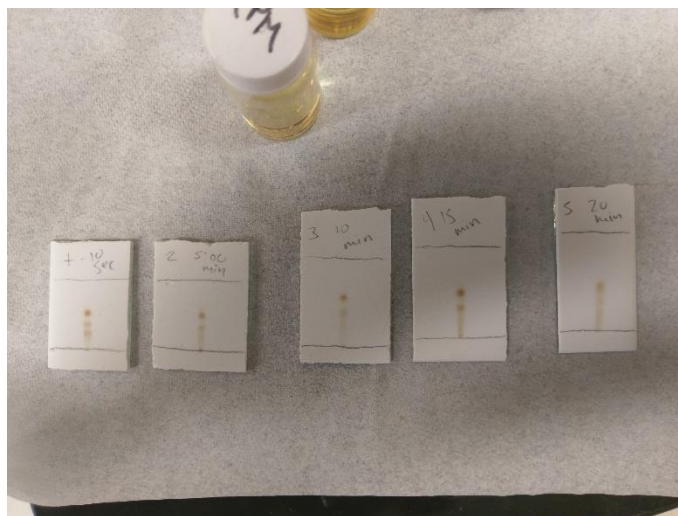


Figure 6.1.1 TLC Monitoring of synthesis of 5,15-dibromo-10,20-diphenyl porphyrin. After 20 minutes only one product was observed and the reaction mixture was quenched.

Once only one product was observed in the reaction mixture, the reaction was quenched with acetone and the solvent removed by rotary evaporation. Following rotary evaporation, the recovered purple solid was placed atop a vacuum filtration set up and washed with several portions of cold methanol. The product was characterized by ¹H-NMR (see Figure 6.1.2).

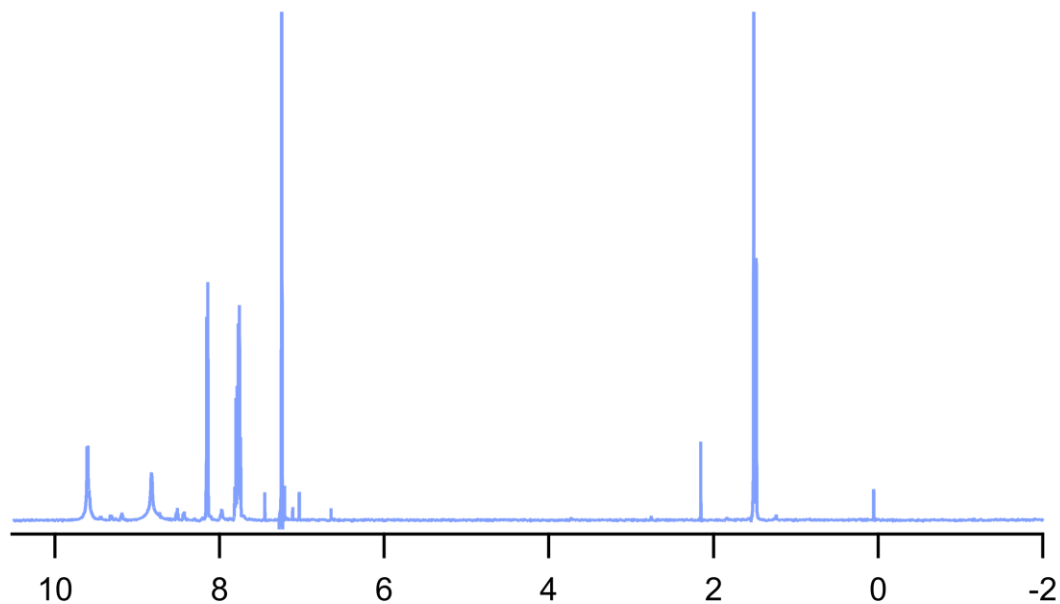


Figure 6.1.2 $^1\text{H-NMR}$ Spectrum of 5,15-dibromo-10,20-diphenyl porphyrin (CDCl_3 , δ : -2.81 (s, 2 H), 7.80 (m, 6H), 8.17 (dd, 4H), 8.85 (d, 4H), 9.63 (d, 4H))

Zinc insertion into the porphyrin ring was then attempted by the following procedure: 5,15-dibromo-10,20-diphenyl porphyrin and zinc acetate dihydrate were combined in chloroform/methanol 10:3 and allowed to reflux for 2 hr. Following reflux, the solvent was removed by rotary evaporation. The product was washed in an identical manner to the 5,15-dibromo-10,20-diphenyl porphyrin with the addition of several washings with cold distilled water.

Prior to this method, an alternate synthesis was attempted and was deemed largely unsuccessful. In this attempt, 5,15-dibromo-10,20-diphenylporphyrin and zinc chloride were allowed to reflux for 2 hr in dimethylformamide (DMF). After reflux, it was determined to be too laborious to remove the solvent by rotary evaporation due to the high boiling point of DMF. Instead, the reaction mixture was gravity filtered. Some solid was recovered, but most of the reaction mixture passed directly through the filter and recovery of the solid off the filter paper was very low.

Ultimately, zinc insertion to the di-brominated porphyrin was too difficult, perhaps due to bromine changing the basicity of the porphyrin species and its subsequent reactivity with the Lewis acid Zn^{2+} . Furthermore, two bromine sites could be problematic when carrying out the Kumada coupling, as aniline could attach at both the 5 and 15 positions. Therefore, a monobromination¹³ approach was then carried out.

To begin, DPP (20 mg, 43 μ mol) and NBS (6 mg, 33 μ mol) were dissolved in chloroform (22 mL) stirred and cooled in an ice bath at ~ 0 °C for 30 min. The solvent was then removed by rotary evaporation and the product was washed with several portions of cold methanol. The product was analyzed by 1H -NMR (Figure 6.1.3).

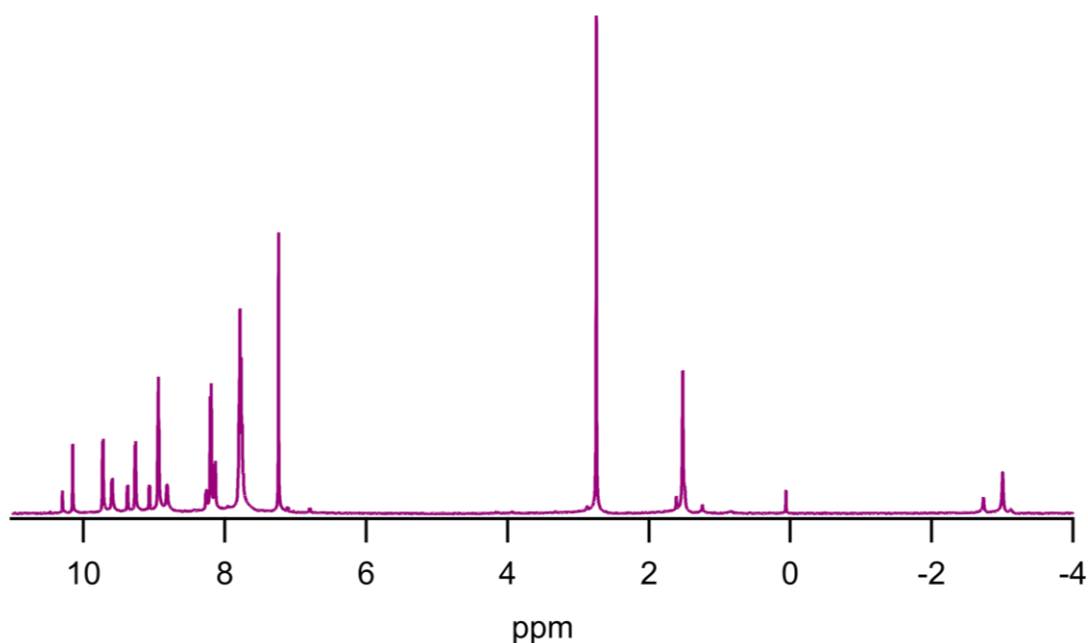


Figure 6.1.3 1H -NMR Spectrum of 5-bromo-10,20-diphenyl porphyrin ($CDCl_3$, $\delta = 10.16$ (s, 1H), 9.71 (d, 2H), 9.24 (d, 2H), 8.95 (d, 4H), 8.21 (dd, 4H), 7.80 (m, 6H), - 3.01 (s, 2H))

Following confirmation of the monobrominated product, the zinc complex was synthesized via reaction of the product with ~ 10 molar equivalents of zinc acetate in chloroform/methanol (10:30 at room temperature for 1 hr. An NMR spectrum was

obtained of this compound. The disappearance of the negative peak attributed to the internal ring hydrogens observed in 5-bromo-10,20-diphenyl porphyrin confirmed successful zinc insertion (See Figure 6.1.4)

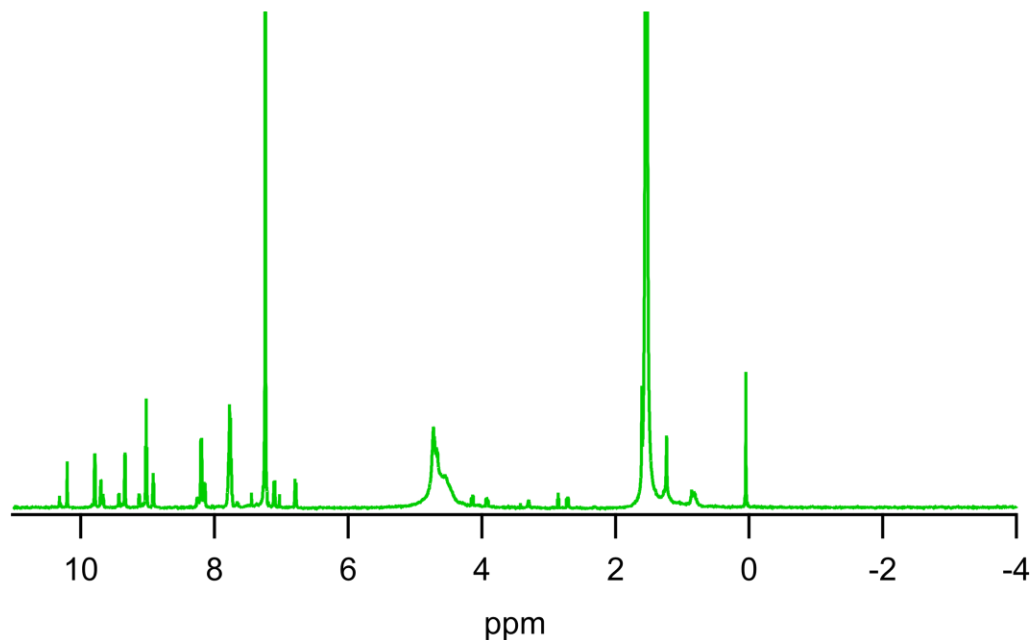


Figure 6.1.4 $^1\text{H-NMR}$ Spectrum of $\text{Zn}(5\text{-bromo-10,20-diphenyl porphyrin})$ (CDCl_3 , $\delta = 10.24$ (s, 1H), 9.81 (d, 2H), 9.37 (d, 2H), 8.95 (d, 4H), 8.25 (dd, 4H), 7.80 (m, 3H), 7.27 (m, 3H)). The disappearance of the negative peak attributed to the internal ring hydrogens observed in 5-bromo-10,20-diphenyl porphyrin confirmed successful zinc insertion Note: peak at 1.56 is water contamination.

Upon successful synthesis of the monobrominated zinc porphyrin complex, a Kumada coupling was attempted to insert an aniline at the 5 or 15 position.¹³ $\text{Zn}(5\text{-bromo-10,20-diphenylporphyrin})$ (9 mg) and $\text{NiCl}_2(\text{dppe})$ (2 mg) were combined in a schlenk flask with a reflux condenser and purged under argon. Extra dry THF (10 mL) and 4- bis(trimethylsilyl)amino phenylmagnesium bromide (1 mL) were added through a rubber septum. The reaction was left to reflux for 24 hr.

Following reflux, the reaction was quenched with a small volume (2–3 mL) of isopropyl alcohol. A workup was attempted with water to separate the aqueous and organic layer. This was a grave oversight as THF and water are infinity miscible. The

solvent was instead rotary evaporated. No quantitative yield was recovered from this reaction. This was likely due to a small amount of the initial monobrominated porphyrin starting material and a flawed work-up. The desired product of this reaction is displayed in Figure 6.1.5

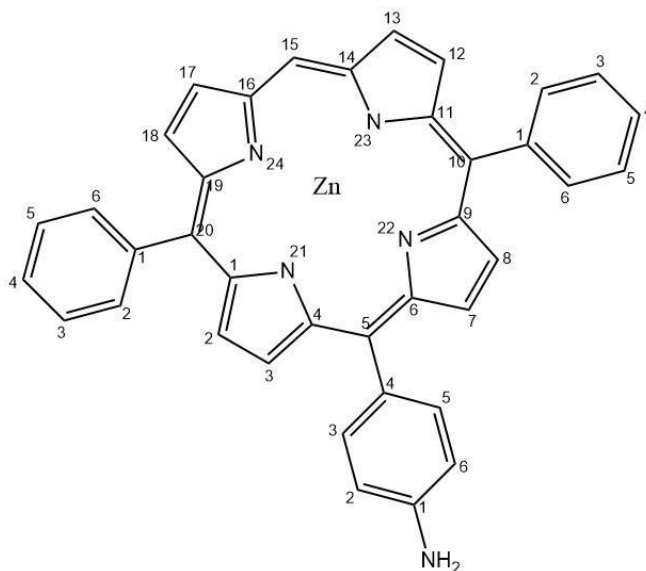


Figure 6.1.5 Desired product of Kumada Coupling an aminophenyl group was intended to be attached at the 5 position of DPP

With the Kumada coupling ultimately being unsuccessful, research efforts turned towards exploring tetra-substituted porphyrins for the single molecule organic PV as DPP is difficult to synthesize from starting materials, expensive to purchase, and the reactions involving it tend to be riddled with side reactions and bear low quantitative yields. Using tetra-substituted porphyrins is, in essence, achieving the same overall result as the chemistry with DPP was trying to achieve, but the starting materials are much cheaper and commercially available. The Walter synthesis was chosen for this reason and it introduces further control over the positions of reaction because the asymmetric design of the molecule prevents reaction at multiple available positions.

6.2 Discussion and Conclusions of Experiments with Tetraphenyl Substituted Porphyrins and Surface Experiments

6.2.1 Yield and Purification

The reasons for choosing an asymmetrically substituted tetraphenyl porphyrin have already been explained above in §2.5 therefore, this section will discuss challenges in the synthesis and purification of the desired porphyrin, *trans*-TA₂CM₂PP.

As with much chemistry involving porphyrins, the results of our experiments were plagued by poor yield and separation challenges. The best yield for the *trans*-TA₂CM₂PP synthesis attempts was about 61% which is on-par and comparatively very good with yields expected from the Lindsey synthesis of porphyrins. The Lindsey synthesis sees equilibrium established between starting materials and the porphyrinogen macrocycle followed by gentle oxidation by a species such as DDQ. Yields for this synthesis type tend to range from 10–60% and our synthesis is very similar to the Lindsey class of porphyrin synthesis.¹⁴ However, it should be noted that this reported yield is from one synthesis attempt and no purification beyond recrystallization was performed. It is not known if this yield can be consistently achieved. Freshly distilling all organic solvents could potentially decrease side reactions and impurities. Whether or not this improves yield can be tested very easily and weighed against the time input on the distillation process. If distilling organic solvents only marginally improves yield but requires much more time to complete, it is not advisable to carry out this practice.

Perhaps the greatest obstacle in the synthesis of our porphyrins is the purification of the product. Porphyrins are most commonly purified via column chromatography, however, we experienced challenges carrying a column out due to the aforementioned issues with yield. Running a column tended to greatly decrease the amount of product recovered. Furthermore, some of the synthesized porphyrins experienced solubility challenges if very impure and most of the product would simply sit atop the stationary phase and be unable to diffuse through the column. As such, the

main purification technique employed was recrystallization of the product in an appropriate organic solvent. Methanol was most often the chosen solvent for this purpose as porphyrin solubility increases as methanol is heated and then when cooled the solid would precipitate out. A Soxhlet extraction approach could be tried to determine whether that eliminated impurities when removing the solvent. Furthermore, if the synthetic route becomes streamlined but purification challenges still exist, the porphyrin could be purified by high-pressure liquid chromatography (HPLC).

6.2.2 Silicon Surface Experiments

The results of the silicon surface experiments are important for one very concise reason: they demonstrate that a porphyrin-perylene derivative is capable of being surface attached by the synthetic route we have hypothesized. This is beneficial because it eliminates a step in the overall synthesis of the porphyrin solid which limits more purification and yield issues.

When performing XP spectroscopy, the sensitivity factors are used to scale the measured peak areas so that variations in the peak areas are representative of the amount of material on the sample surface. Zinc 2p^{3/2} has a sensitivity factor of 3.354 and Cl 2p has a factor of 0.770 meaning sensitivity to zinc is about 4x more than chlorine and the spectra must be scaled accordingly. The peak area for Zn 2p^{3/2} was calculated to be 1640 eV cps. Therefore, considering the stoichiometry of ZnCl₂, a surface with no successful incorporation of the zinc would see a chlorine 2p peak roughly equivalent to 753 eV cps ($2 * 0.770 / 3.354 * 1640 \text{ eV cps} = 753 \text{ eV cps}$). However, the actual Cl 2p area was calculated to be 102 eV cps (see Figure 6.2.1 for XP spectra)

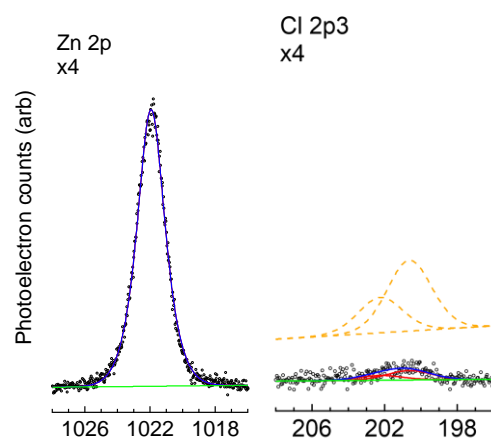


Figure 6.2.1: Comparison of XP spectra from zinc and chlorine on the surface of sample 2 following zinc insertion reaction. The dashed orange traces correspond to an expected quantity of chlorine for ZnCl_2 based on the total zinc signal. The significantly diminished chlorine signal suggests successful incorporation of Zn into the porphyrin with minimal ZnCl_2 remaining on the surface.

The large disparity indicates zinc was incorporated into the surface while the chlorine was not. We interpret the presence of zinc with only a minimal amount of chloride as the incorporation of zinc into the porphyrin macrocycle. This confirms the attachment of the perylene-porphyrin complex to the surface. These surface experiments were done with TAPP, however, since the perylene was reacted with TAPP at one of the aminophenyl groups, by principle it should be able to undergo an identical reaction with of the aminophenyl groups of *trans*- $\text{TA}_2\text{CM}_2\text{PP}$. This is the logical next step of proceeding with this research.

6.3 Future Recommendations

The future of this project looks to address attaching the hole conducting thiophene to the porphyrin, attaching the entire molecule (see Fig. 2.4.5 in §2.5) to a surface, and exploring options for an electrochemical contact at the other end of the cell.

Progress so far on the synthesis of the desired molecule has been promising. The reaction between the porphyrin and the perylene was successful and it was demonstrated that it can adhere to a surface. When considering attaching the thiophene, the recommended procedure would be to adhere the porphyrin-perylene derivative to a

surface and then react the surface with the thiophene to have it attach at the other aminophenyl position of the porphyrin. Attempting to attach the thiophene before surface attaching the porphyrin-perylene derivative could illicit undesired products or introduce major solubility issues.

It is also recommended to investigate both silicon and TiO₂ surfaces. In this MQP, surface experiments were only done on silicon, but the molecule should attach to both surfaces in a similar manner. Preference for a surface type would likely be based on the results of electrochemical experiments and ease of preparation. In the realm of electrochemical properties, much is unknown about the efficiency of the cell, the band positions of the three main components (perylene, porphyrin, and thiophene), and what an appropriate second contact could be. We hypothesize that a Hg liquid contact could be a viable option, but there is a wide parameter space available for investigation.

It is further recommended that more experiments be carried out to test the optical properties of these materials. Techniques such as UV-vis and ultraviolet photoelectron spectroscopy could provide information on these properties and supply a more in depth understanding of our proposed solar cell.

References

1. Baker, A. A History of Solar Cells: How Technology Has Evolved. www.solarpowerauthority.com/a-history-of-solar-cells/
2. Dhar, M. How Do Solar Panels Work?. www.livescience.com/41995-how-do-solar-panels-work.html
3. DiMagno, S. G., Lin, V. S. Y., & Therien, M. J. Facile elaboration of porphyrins via metal-mediated cross-coupling. *J. Org. Chem.* **1993**, 58(22), 5983-5993. doi.org/10.1021/jo00074a027
4. Kangwanwong, T., Pluempanupat, W., Parasuk, W., Keenan, H. E., & Songsasen, A. Using 5,10,15,20-tetra(4-nitrophenyl)porphyrin as a fluorescent chemosensor to determine Ru³⁺. *ScienceAsia*, **2012**, 38(3), 278-282. doi.org/10.2306/scienceasia1513-1874.2012.38.278
5. Karimipour, Gholamreza, Kowkabi, Saeed, & Naghiha, Asghar. New aminoporphyrins bearing urea derivative substituents: synthesis, characterization, antibacterial and antifungal activity. *Braz. Arch. Biol. Technol.*, **2015**, 58(3), 431-442. dx.doi.org/10.1590/S1516-8913201500024
6. Kelber, J.; Bock, H.; Thiebaut, O.; Grelet, E.; Langhals, H. Room-temperature columnar liquid-crystalline perylene imido-diesters by a homogenous one-pot imidification-esterification of perylene-3,4,9,10-tetracarboxylic dianhydride. *Eur. J. Org. Chem.* **2011**, 4, 707-712. doi.org/10.1002/ejoc.201001346
7. Kwiatkowski, J. Organic Photovoltaics: the Good, the Bad, and the Inefficient. www.renewableenergyworld.com/articles/2008/05/organic-photovoltaics-the-good-the-bad-and-the-inefficient-52410.html
8. Latos-Grażyński, L. Porphyrin Basics. www.cpp.edu/~lsstarkey/courses/CHM-Lab/PorphyrinBasics.pdf
9. Milanesio, M. E., Gervaldo, M., Otero, L. A., Sereno, L., Silber, J. J., & Durantini, E. N. Synthesis of a diporphyrin dyad bearing electron-donor and electron-withdrawing substituents with potential use in the spectral sensitization of semiconductor solar cells. *J. Porphyrins and Phthalocyanines* **2003**, 7(1) doi.org/10.1142/S1088424603000070
10. Office of Energy Efficiency and Renewable Energy. Organic Photovoltaics Research. www.energy.gov/eere/solar/organic-photovoltaics-research
11. Ratner, M. A brief history of molecular electronics. England: Nature Publishing Group. **2003**. doi.org/10.1038/nnano.2013.110

12. Sabras, M. History of Solar Power.
www.instituteforenergyresearch.org/renewable/solar/history-of-solar-power/
13. Shanmugathan, S, Johnson, C., Edwards, C., Matthews, K., Dolphin D., Boyle, R. Regioselective halogenation and palladium-catalysed couplings on 5,15-diphenylporphyrin. *J. Porphyrins Phthalocyanines* **2000**. 4. 228-232.
[doi.org/10.1002/\(SICI\)1099-1409\(200004/05\)4:33.3.CO;2-Z](https://doi.org/10.1002/(SICI)1099-1409(200004/05)4:33.3.CO;2-Z)
14. Shy, H., Mackin, P., Orvieto, A. S., Gharbharan, D., Peterson, G. R., Bampos, N., & Hamilton, T. D. The two-step mechanochemical synthesis of porphyrins. *Faraday Discuss.* **2014**, 170, 59–69. doi.org/10.1039/c3fd00140g
15. Spooner, E. Organic Photovoltaics vs 3rd-Generation Solar Cell Technologies.
www.ossila.com/pages/organic-photovoltaics-vs-3rd-gen-solar-tech
16. Tripathy, S. Organic Semiconductor 3,4,9,10-Perylenetetracarboxylic dianhydride (PTCDA). U of Cincinnati 2002.
pdfs.semanticscholar.org/aed0/5a09025e93cf2da46679cf6eec73333325e9.pdf
17. Walter, M. Nanostructured aminophenylporphyrin films for use in bulk heterojunction and inverse dye-sensitized TiO₂ solar cells. Ph.D. Thesis, Portland State University, Portland, OR, 2008.
pqdtopen.proquest.com/doc/304498342.html?FMT=ABS
18. Walter, M., Wamser, C. C., Ruwitch, J., Zhao, Y., Braden, D., Stevens, M., . . . Pessiki, P. J. Syntheses and optoelectronic properties of amino/carboxyphenylporphyrins for potential use in dye-sensitized TiO₂ solar cells. *J. Porphyrins Phthalocyanines* **2007**, 11(8), 601-612. doi.org/10.1142/s1088424607000709
19. Yadav, Omprakash & Varshney, Atul & Kumar, Anil. Manganese(III) mediated synthesis of A₂B Mn(III) corroles: A new general and green synthetic approach and characterization. *Inorg. Chem. Commun.* **2007**. 86.
doi.org/10.1016/j.inoche.2017.10.018

7. Appendix A: $^1\text{H-NMR}$ of CDCl_3

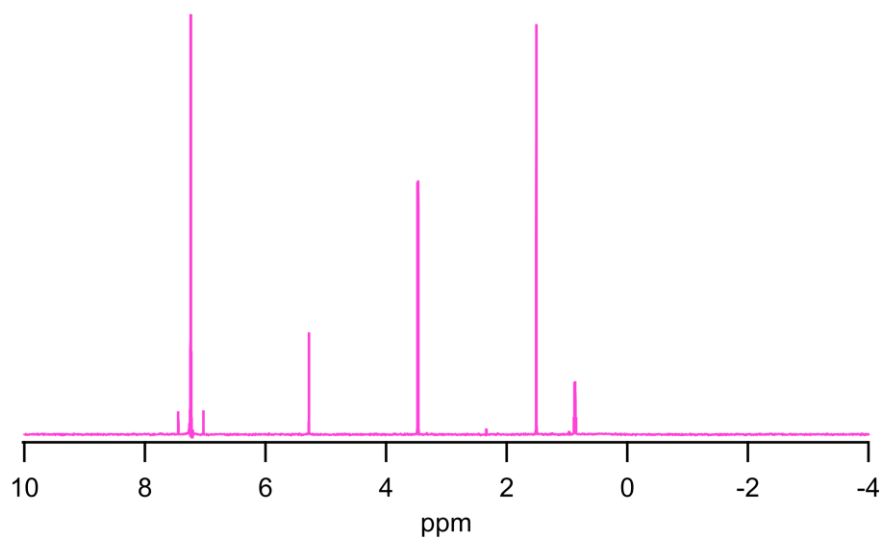


Figure A1: $^1\text{H-NMR}$ Spectrum of CDCl_3 to illustrate contaminants. CDCl_3 peak is at 7.26 ppm
1.56 ppm-Water, 2.17ppm-Acetone, 3.49ppm-Methanol, 5.30ppm-DCM, 7.07ppm-unknown,
7.47ppm-unknown